Optimizaton of Mo-Si-B Intermetallic Alloys

J.H. SCHNEIBEL, R.O. RITCHIE, J.J. KRUZIC, and P.F. TORTORELLI

Mo-Si-B intermetallics consisting of the phases Mo_3Si and Mo_5SiB_2, and a molybdenum solid solution ("α-Mo"), have melting points on the order of 2000 °C. These alloys have potential as oxidation-resistant ultra-high-temperature structural materials. They can be designed with microstructures containing either individual α-Mo particles or a continuous α-Mo phase. A compilation of existing data shows that an increase in the volume fraction of the α-Mo phase increases the room-temperature fracture toughness at the expense of the oxidation resistance and the creep strength. If the α-Mo phase could be further ductilized, less α-Mo would be needed to achieve an adequate value of the fracture toughness, and the oxidation resistance would be improved. It is shown that microalloying of Mo-Si-B intermetallics with Zr and the addition of $MgAl_2O_4$ spinel particles to Mo both hold promise in this regard.

I. INTRODUCTION

THE design of structural materials with properties exceeding those of nickel-base superalloys presents considerable challenges. First, the melting point of such materials needs to be well above that of nickel-base superalloys. Second, a sufficient degree of oxidation resistance is required. Third, the service temperature for creep needs to be significantly higher than that for nickel-base superalloys. Fourth, the fracture toughness must be adequate. The number of materials systems with the potential to meet all of these requirements is limited. Presently, niobium silicides, molybdenum borosilicides, and precious metal superalloys are the main metallic systems under investigation.[1] Each of these systems has its merits. For example, niobium silicides have a relatively low density and tend to be ductile at room temperature. Molybdenum borosilicides exhibit some degree of oxidation resistance as long as the volume fraction of α-Mo (the solid solution Mo phase) is not too high. Precious metal superalloys are oxidation resistant and amenable to the same strengthening mechanism as γ-γ' nickel-base superalloys. However, these systems also have significant disadvantages. Niobium-based systems suffer from poor oxidation resistance. Molybdenum-based systems have a relatively high density and marginal ductility, and, for low Si and B concentrations, they suffer from poor oxidation resistance. Precious metal superalloys exhibit very high densities and are very expensive. Clearly, there are no simple answers in the quest to find materials systems with properties beyond those of nickel-base superalloys.

J.H. SCHNEIBEL, Senior Research Staff Member, and P.F. TORTORELLI, Group Leader, are with the Metals and Ceramics Division, Oak Ridge National Laboratory, Oak Ridge, TN 37831. Contact e-mail: schneibeljh@ornl.gov R.O. RITCHIE, Professor, is with the Materials Sciences Division, Lawrence Berkeley National Laboratory, and Department of Materials Science and Engineering, University of California, Berkeley, CA 94720. J.J. KRUZIC, Assistant Professor, is with the Department of Mechanical Engineering, Oregon State University, Corvallis, OR 97331-6001.

This article is based on a presentation made in the symposium entitled "Beyond Nickel-Base Superalloys," which took place March 15–17, 2004, at the TMS Spring meeting in Charlotte, NC, under the auspices of the SMD-Corrosion and Environmental Effects Committee, the SMD-High Temperature Alloys Committee, the SMD-Mechanical Behavior of Materials Committee, and the SMD-Refractory Metals Committee.

This article focuses on molybdenum borosilicide alloys containing a molybdenum solid solution phase to provide toughening and builds on our earlier work on this topic.[2] Mo-Si-B alloys containing α-Mo were pioneered by Berczik.[3,4] Figure 1 shows the appropriate section of the Mo-Si-B phase diagram.[5] The alloys considered in the present work are all in the Mo-Mo_3Si-Mo_5SiB_2 phase triangle highlighted in Figure 1. Mo_3Si exhibits the A15 crystal structure and is brittle.[6] Its equilibrium silicon concentration is 0.5 or 1 at. pct lower than the stoichiometric value.[6,7] Mo_5SiB_2 ("T2") exhibits a tetragonal crystal structure with the Cr_5B_3 structure type, with 32 atoms in the unit cell; like Mo_3Si, it is brittle.[8]

The goal of this article is twofold. First, based on existing data, the dependence of properties such as oxidation resistance, fracture toughness, ductility, and creep strength on the volume fraction and distribution of the α-Mo phase will be summarized. Second, ways to improve the room-temperature ductility of the α-Mo phase will be discussed. If this ductility can be improved, the volume fraction of α-Mo needed to achieve the required level of fracture toughness will be reduced, thereby allowing for improved oxidation resistance.

II. EXPERIMENTAL PROCEDURES

In order to assess the toughening effects of up to 3 at. pct Zr additions, Mo-Zr-Si-B alloys were prepared by arc melting elemental starting materials in a partial pressure of argon (70 kPa) on a water-cooled copper hearth. The purities of the starting materials Mo, Si, B, and Zr were 99.95, 99.99, 99.5, and 99.5 wt pct, respectively. The alloy compositions were Mo-12Si-8.5B-xZr, where x is 0 to 3 at. pct. Unless stated otherwise, alloy compositions will be given in atomic percent. The alloys were remelted several times in order to improve their homogeneity and drop cast into cylindrical water-cooled copper molds with a diameter of 12.5 mm. Bend bars with a cross section of 3 × 4 mm were electrodischarge machined. They were chevron-notched at midlength with a diamond blade producing approximately 100-μm-wide cuts. The resulting triangular area holding the specimen together in its middle was approximately 3-mm wide and 2-mm high. The chevron-notched specimens were tested in three-point bending with a loading span of 20 mm

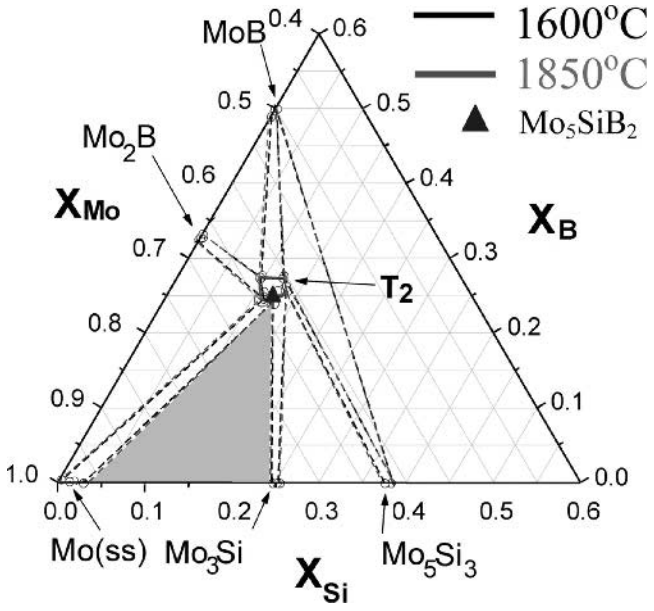

Fig. 1—Ternary Mo-Si-B phase diagram with axes given in atomic fractions.

and a crosshead speed of 10 μm/s. A provisional fracture toughness K_q was determined from the relationship[9]

$$K_q = [EG/(1 - \nu^2)]^{1/2} \quad [1]$$

where E is Young's modulus, $G = W/A$ is the work W expended during fracture divided by the area A swept out by the crack, and ν is Poisson's ratio. The fracture toughness values determined with this technique tend to be somewhat higher than those determined with more rigorous techniques. On the other hand, this technique requires less sample material, is simpler to implement than more rigorous techniques, and is considered suitable for comparative purposes.

Additionally, the effect of 9 vol pct of $MgAl_2O_4$ spinel particles on the ductility of molybdenum was assessed using Mo powder (2 to 8 μm) that was hot pressed with and without $MgAl_2O_4$ spinel particles (-325 mesh, <45 μm) *in vacuo* (mechanical pump) in a graphite die for 4 hours at 1800 °C and a pressure of 21 MPa. Bend bars with a cross section of 3×4 mm were fabricated from the hot-pressed coupons by electrodischarge machining and grinding with SiC paper to a 600-grit final finish. They were tested at room temperature in a three-point bending fixture, again with a loading span of 20 mm and a crosshead speed of 10 μm/s.

Metallography specimens were prepared by grinding, mechanical polishing, and etching in Murakami's reagent. Microstructural examination was carried out by optical microscopy as well as by scanning electron microscopy (SEM).

III. RESULTS AND DISCUSSION

A. *Processing and Microstructure of Mo-Si-B Alloys*

The microstructures of Mo-Si-B alloys are characterized by three parameters. First, the morphology is important, *i.e.*, whether the α-Mo phase occurs in the form of discontinuous particles in a continuous Mo_3Si-Mo_5SiB_2 matrix, or whether particles of Mo_3Si-Mo_5SiB_2 are distributed in a continuous matrix of α-Mo. Although a third morphology of interpenetrating continuous networks of α-Mo and intermetallic is feasible, it is not discussed here. Second, the volume fraction of the toughening α-Mo phase is of key importance. Third, the size scale of the α-Mo phase is significant. Figure 2(a) shows the microstructure of cast and annealed Mo-12Si-8.5B.[10] The α-Mo (the bright phase) is distributed in the form of large primary and small secondary particles in a matrix consisting of Mo_3Si and Mo_5SiB_2. One can also produce microstructures in which the α-Mo is continuous.[11] This may, for example, be achieved by casting a Mo_3Si-Mo_5SiB_2 intermetallic with the composition Mo-20Si-10B (which is a mixture of Mo_3Si and Mo_5SiB_2), crushing it into powder, and then vacuum annealing it. Vacuum annealing of the powder for hours or days at 1600 °C removes the Si as volatile SiO or Si vapor and leaves a Mo-rich coating behind. The resulting Mo-coated powder is then consolidated by hot-isostatic pressing. Figure 2(b) illustrates such a microstructure.[2] By varying the particle size of the crushed powder and the time of annealing, the scale and volume fraction of the α-Mo phase can be

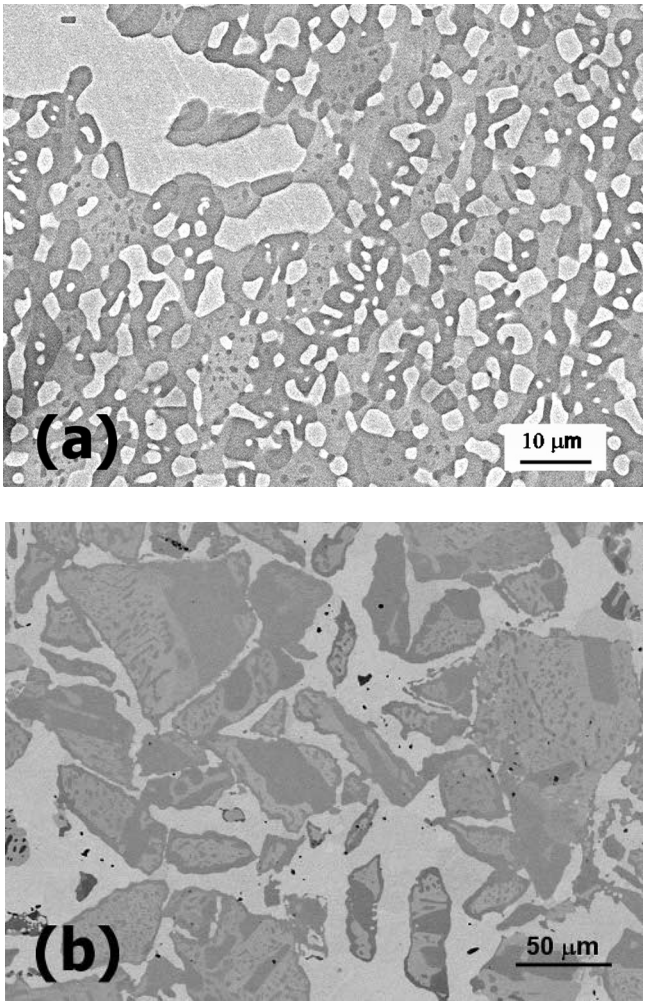

Fig. 2—SEM micrographs of (*a*) Mo-12Si-8.5B, arc-cast followed by annealing for 24 h at 1600 °C; and (*b*) Mo-Si-B consolidated from vacuum-annealed Mo-20Si-10B powders by hipping for 4 h at 1600 °C and 207 MPa (30 ksi). The α-Mo volume fractions (bright phase) are 42 and 34 vol pct, respectively.

engineered within a wide range. For example, the size scale of the α-Mo phase in Figure 2(b) is much coarser than that in Figure 2(a), thus illustrating the flexibility of microstructural design of these alloys.

B. *Oxidation Resistance of Mo-Si-B Alloys*

Akinc *et al.*[12] have identified the substantial improvement in the oxidation resistance of molybdenum silicides by boron additions. Even when an alloy contains α-Mo, boron can improve the oxidation resistance substantially. A common feature of the oxidation behavior of these alloys is an initial region of fast mass loss followed by a region of much slower mass change. The initial mass loss is due to the rapid evaporation of Mo as MoO_3. Once a sufficient quantity of MoO_3 has evaporated, the Si and B concentration on the surface becomes high enough to form a protective borosilicate film. Figure 3 illustrates the fast initial weight loss for two Mo-Si-B alloys with different α-Mo volume fractions.[2] Both alloys were hot-isostatically pressed ("hipped") from powders subjected to the Si evaporation process in order to make the α-Mo matrix approximately continuous. As expected, the rate of the mass loss increases as the α-Mo volume fraction increases. Figure 4 shows mass loss data as a function of the α-Mo volume fraction. The filled circles correspond to cast and annealed microstructures containing individual α-Mo particles and were obtained with a single 24-hour cycle.[13,14] The open circles (Reference 2 and Figure 3) are for a nominally continuous α-Mo matrix and correspond to 20 one-hour cycles at 1200 °C. The squares correspond to cyclic oxidation at 1300 °C in air.[15] Since the oxidation rates at 1300 °C are similar to those at 1200 °C,[13] the scatter in the data is unlikely to be caused by the difference in the two temperatures. There are other factors that can introduce variations in the oxidation rate. For example, Supatarawanich *et al.*[15] found that the oxidation resistance at 1300 °C was improved if the Mo_3Si/T2 ratio was increased. They also found that the measured volume fraction depended on the particular technique employed; point counting on metallographic cross sections usually resulted in higher α-Mo volume fractions than calculations based on the isothermal 1600 °C phase diagram. In view of all these confounding variables, it is difficult to verify whether the oxidation rates of specimens with continuous α-Mo are significantly higher than those of specimens with discontinuous α-Mo. The purpose of the data is mainly to serve as a guide for further work. Again, it is worth pointing out that after the initial mass loss, the rate of oxidation decreases significantly, *i.e.*, mass loss rates obtained after the initial fast loss will be much smaller than those implied by Figure 4. This suggests that surface treatment to promote a borosilicate layer prior to service may reduce some of the detrimental effects that a high α-Mo content has on the oxidation resistance.

C. *Mechanical Properties of Mo-Si-B Alloys*

1. *Creep strength*

Figure 5 shows the dependence of the compressive creep strength of Mo-Si-B alloys on the α-Mo volume fraction. The creep strengths were defined as the stress reached at 2 pct

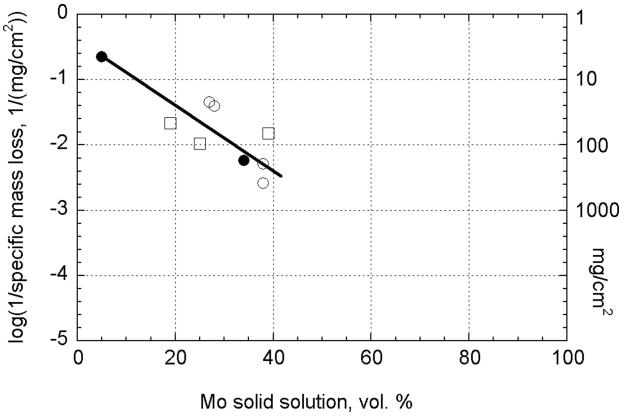

Fig. 4—Specific mass loss of Mo-Si-B alloys after oxidation for 20 to 24 h at 1200 °C and 1300 °C in air, as a function of α-Mo volume fraction. The black dots correspond to specimens containing individual α-Mo particles, tested at 1200 °C; the open circles correspond to specimens with a continuous α-Mo matrix tested at 1200 °C; and the squares correspond to cast specimens tested at 1300 °C.

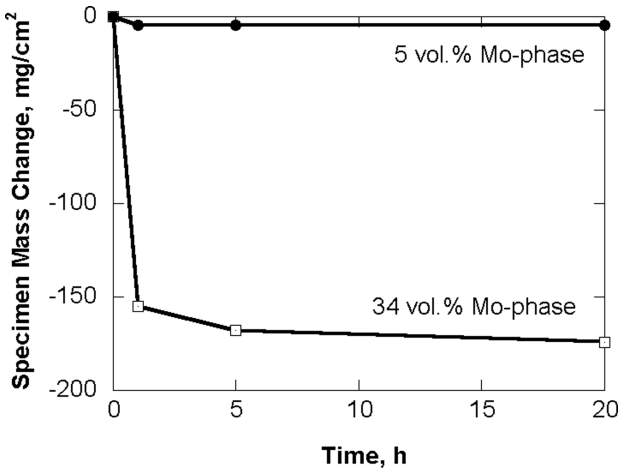

Fig. 3—Cyclic oxidation of Mo-Si-B alloys with different α-Mo volume fractions, at a temperature of 1200 °C and for 1-h cycles. The alloys were hipped Mo-20Si-10B powders (45 to 90 μm) that were vacuum annealed for different times to produce different α-Mo volume fractions.

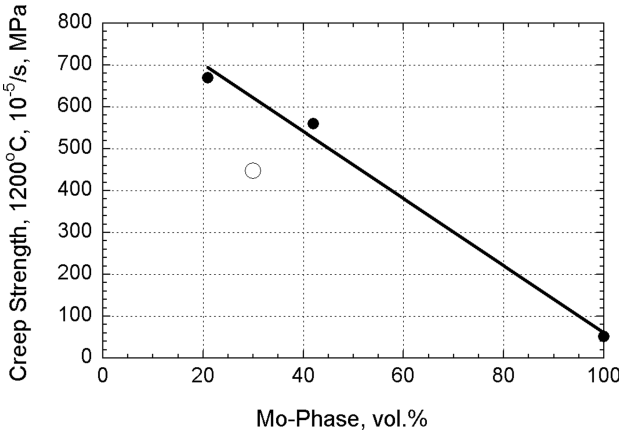

Fig. 5—Creep strength of Mo-Si-B alloys at 1200 °C as a function of the α-Mo volume fraction. The black dots correspond to specimens containing individual α-Mo particles, as well as pure Mo; and the circle to a specimen with a continuous α-Mo matrix.

plastic deformation in constant displacement experiments with an initial strain rate of 10^{-5} s^{-1}. For simplicity, the potential effect of the Mo_3Si/T2 ratio on the creep strength has been ignored. The black dots correspond to microstructures with individual α-Mo particles, as well as a pure Mo specimen, and have been fitted by a straight line, while the open point corresponds to a continuous α-Mo phase.[10] The creep strength of pure Mo was extrapolated from creep experiments carried out at 1200 °C and 69 MPa, which resulted in a strain rate of 6×10^{-5} s^{-1}.[16] As can be seen, a decrease in the α-Mo volume fraction, *i.e.*, an increase in the Mo_3Si-Mo_5SiB_2 volume fraction, gives rise to substantial creep strengthening. If the α-Mo is present in the form of a continuous matrix, the creep strength is relatively low (open circle in Figure 5).

One tensile creep test was carried out at 1200 °C in argon, for a material with the composition Mo-12Si-8.5B containing discontinuous α-Mo.[17] The stress was ramped up in three steps, until the specimen fractured at a plastic strain of 2.5 pct. The creep rates observed for the different applied stresses are listed in Table I.

It should be pointed out that alloying additions can increase the creep strength significantly. Compression tests showed that partial substitution of Mo with 19.5 at. pct Nb increases the creep strength by approximately a factor of 2.[10]

2. *Ductility*

To date, not many tensile tests have been reported for Mo-Si-B alloys. A cast and annealed Mo-12Si-8.5B specimen tested in flowing nitrogen at 1520 °C fractured at a plastic strain of 0.3 pct.[18] This alloy contained approximately 40 vol pct of particulate α-Mo in a Mo_3Si-Mo_5SiB_2 matrix. Its low ductility is probably due to the presence of the continuous, brittle Mo_3Si-Mo_5SiB_2 matrix. For a continuous α-Mo phase, higher ductility values are expected. Indeed, an alloy with 49 vol pct of continuous α-Mo matrix exhibited a fracture strain of 1.8 pct at 1200 °C in vacuum.[19]

3. *Room-temperature fracture toughness*

A major difference of Mo-Mo_3Si-Mo_5SiB_2 intermetallics, as compared to typical structural ceramics, is the presence of the ductile α-Mo phase. Figure 6 illustrates the pronounced increase in the room-temperature fracture toughness as the α-Mo volume fraction increases; details of the data are listed in Table II. For a continuous α-Mo matrix with a large size scale, Kruzic *et al.*[19] showed that substantial initiation fracture toughness values and pronounced *R*-curve behavior can be obtained. For a specimen containing 49 vol pct of continuous Mo phase, an initiation toughness of $12\ MPa\sqrt{m}$ was measured, while a maximum value of $21\ MPa\sqrt{m}$ was reached after ~3 mm of stable crack extension (Figure 6). Unfortunately, the extremely high fracture toughness values afforded by these high α-Mo volume fractions are accompanied by a serious degradation in the oxidation resistance (Figure 4).

Table I. Tensile Creep Rates for Mo-12Si-8.5B at 1200 °C

Stress, MPa	Strain Rate, s^{-1}
50	2.1×10^{-8}
75	4.5×10^{-8}
100	1.4×10^{-7}

In general, high fracture toughness values are achieved with a large volume fraction of a continuous, coarse α-Mo phase. Good oxidation resistance is achieved by low volume fractions of α-Mo. The requirements for high fracture toughness thus run opposite to those for good oxidation resistance. If the ductility and fracture toughness of the α-Mo phase could be improved, less α-Mo would be required to obtain a Mo-Si-B alloy with satisfactory fracture toughness and ductility. A smaller volume fraction of α-Mo, in turn, would result in an improved oxidation resistance of the alloy (Figure 4).

Figure 7 shows an SEM micrograph of the fracture surface of a high-toughness Mo-Si-B specimen with 49 vol pct of continuous α-Mo (Figure 6). The micrograph shows regions of cleavage fracture that correspond mostly to fracture of the Mo_3Si and Mo_5SiB_2 intermetallic particles, while the α-Mo phase exhibits a large percentage of intergranular fracture. It is likely that its ductility will increase if the incidence of intergranular fracture can be minimized. Therefore, there is potential for improving the already high fracture toughness of this alloy even further. In Section D, several possibilities for improving the ductility of the α-Mo phase will be discussed, and exploratory experimental work will be presented.

D. *Improving the Ductility of the α-Mo Phase*

1. *Mo ligament size*

Materials with bcc crystal structures, such as Mo, often fail by cleavage. Cleavage fracture can be nucleated by the high stresses ahead of dislocation pileups. If the material thickness is smaller than the length of the pileups required to nucleate a cleavage crack, cleavage fracture will not occur. This has been demonstrated for the room-temperature fracture of FeAl ligaments in FeAl composites containing TiC particulates.[23] Ligaments thicker than 1 to 2 μm showed limited necking, but fracture occurred ultimately by cleavage. In ligaments thinner than 1 to 2 μm, ductile chisel-type fracture occurred. It is conceivable that a similar transition occurs in the α-Mo phase in Mo-Si-B alloys. The change in fracture mode is expected to improve the energy dissipation and the fracture toughness. However, the effective-

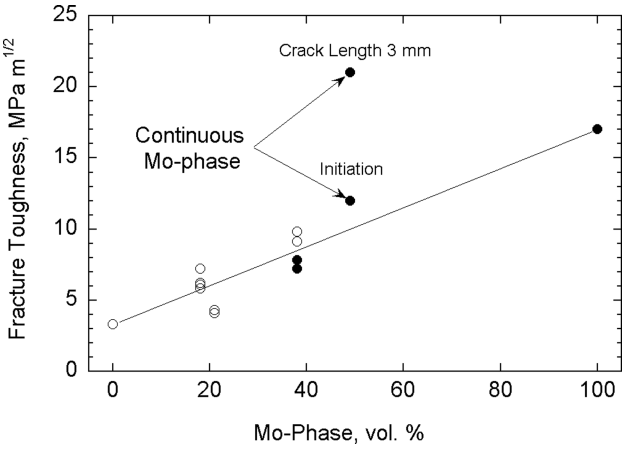

Fig. 6—Room-temperature fracture toughness as a function of the α-Mo volume fraction. Full and open symbols denote standard and nonstandard tests, respectively (Table II).

Table II. Room-Temperature Fracture Toughness Data for Mo-Si-B Intermetallic Alloys

Composition, At. Pct	α-Mo, Vol Pct	Test Method	Fracture Toughness, $MPa\sqrt{m}$	Reference
Mo-18.2Si-13.6B	0	Chevron-notch specimen	3.3	14
Mo-15.3Si-11.5B	18 (discontinuous)	Chevron-notch specimen	6.2, 5.8, 6.1, 7.2	14
Mo-16.8Si-8.4B	21 (discontinuous)	indentation; razor micronotch	4.1, 4.3	21
Mo-12Si-8.5B	38 (discontinuous)	Chevron-notch specimen	9.1, 9.8	14
Mo-12Si-8.5B	38 (discontinuous)	precracked disk compact tension	7.2, 7.8 (after crack advance)	22
	49 (continuous)	precracked disk compact tension	12; 21 (after 3-mm crack advance)	19
Mo-1 wt pct Zr	100 (continuous)	similar to ASTM E399	17	20

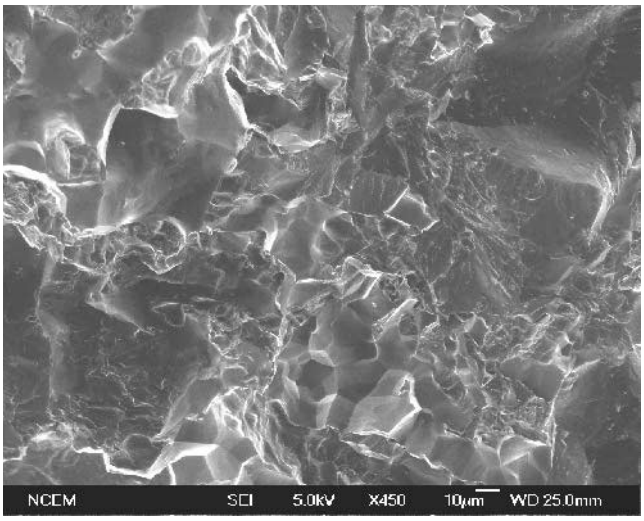

Fig. 7—SEM micrograph of fracture surface of Mo-Si-B alloy with 49 vol pct continuous α-Mo. The initiation fracture toughness for this alloy was $12\ MPa\sqrt{m}$; a value of $21\ MPa\sqrt{m}$ was reached after the crack propagated 3 mm (Fig. 6).

ness of ductile-phase toughening decreases with decreasing ligament size.[24] Therefore, when the thickness of the α-Mo ligaments decreases, the overall fracture toughness of a Mo-Mo_3Si-Mo_5SiB_2 alloy is determined by two competing processes: the increase in the fracture toughness due to the transition from cleavage to chisel-type fracture, and the decrease in the fracture toughness caused by the decreasing thickness of the ligaments. Therefore, this mechanism can give, at best, an arrest in the general decrease of the fracture toughness as the ligament size of the toughening phase is decreased.

2. *Microalloying additions*

As shown by Kumar and Eyre,[25] the room-temperature ductility of molybdenum is sensitive to interstitials such as oxygen and carbon. If the grain boundaries contain too much oxygen, intergranular fracture occurs and the ductility decreases. Wadsworth *et al*.[26] pointed out that the atomic ratio of C/O must be greater than 2 for satisfactory ductility to occur. While the effects of carbon and oxygen interstitials on the α-Mo phase in Mo-Si-B alloys have not been studied to date, it is well known that additions of reactive elements such as Zr and Ti are beneficial for the mechanical properties of molybdenum alloys such as TZM (Mo-0.5Ti-0.1Zr, wt pct). These reactive elements getter interstitials such as C and O (although it is not clear in which way they would influence the C/O ratio). They are typically added as microalloying additions, *i.e*., with concentrations on the order of 1 at. pct or less. In order to determine whether Zr might be beneficial for the fracture toughness of Mo-Si-B alloys, Mo-12Si-8.5B (Figure 2(a)) was alloyed with up to 3 at. pct Zr, where the Zr was expected to substitute for Mo. In order to determine the trends in the fracture toughness, three-point flexure tests with chevron-notched specimens were carried out as described previously. While the values obtained from these tests are not rigorous, they provide the trend in the fracture toughness as a function of the Zr concentration. The detailed data for the chevron-notched flexure tests are listed in Table III. Figure 8 shows that the fracture toughness reaches a maximum at approximately 2 at. pct Zr. The exact reasons for the improvement in the fracture toughness are not known at this time. Since it is unlikely that the Zr additions would improve the toughness of the brittle Mo_3Si and T2 phases, it is suggested that the fracture toughness improvement is due to an improvement in the ductility of the α-Mo phase. A titanium addition of 1.5 at. pct, on the other hand, did not increase the fracture toughness noticeably—the value for Mo-12Si-8.5B was $9.0 \pm 0.8\ MPa\sqrt{m}$ and that for Mo-1.5Ti-12Si-8.5B was $10.0 \pm 0.8\ MPa\sqrt{m}$.[27]

3. *$MgAl_2O_4$ spinel additions*

Recently, Brady *et al*.[28] reinvestigated a ductilizing mechanism for chromium that was pioneered by Scruggs *et al*.[29] in the 1960s. When a few vol pct of MgO particles are added to Cr powder, the MgO transforms to $MgCr_2O_4$ spinel during subsequent powder-metallurgical (PM) processing. At room temperature, Cr with spinel particles is more ductile than "pure" Cr. This is counterintuitive since addition of brittle oxide particles would be expected to embrittle the Cr even further. Scruggs attributed the ductility improvement to the gettering of residual nitrogen by the spinel and the accompanying purification of the matrix. Although Brady *et al*.[28] concur that gettering of nitrogen is involved in the ductilization of the Cr, they could not find nitrogen within the spinel particles themselves. Rather, the nitrogen appeared to be segregated at the particle-matrix interfaces. Also, since other nonductilizing oxide dispersions also showed nitrogen segregation, additional factors must be involved in the ductilization.

Scruggs also applied his method to Mo[30] and found that its room-temperature ductility could be improved by addition of $MgAl_2O_4$ spinel particles. A preliminary experiment was carried out with PM-processed Mo and Mo-9 vol pct $MgAl_2O_4$ spinel. Figure 9 illustrates that the spinel-containing Mo exhibits larger flexure ductility than the nominally pure

Table III. Fracture Toughness K_q of Mo-Si-B Alloys Microalloyed with Zr

Nominal Composition At. Pct	Area of Triangle Broken during Test, mm^2	Absorbed Energy, mJ	G, J/m^2	K_q, $MPa\sqrt{m}$	K_q, $MPa\sqrt{m}$, Average ± Standard Deviation
Mo-12Si-8.5B	2.94	0.68	231	9.1	9.0 ± 0.8
Mo-12Si-8.5B	2.88	0.775	267	9.8	
Mo-12Si-8.5B	3.19	0.603	189	8.2	
Mo-12Si-8.5B-1Zr	2.82	1.09	432	12.4	
Mo-12Si-8.5B-1.5Zr	3.05	1.575	516	13.6	13.5 ± 0.7
Mo-12Si-8.5B-1.5Zr	2.89	1.32	457	12.8	
Mo-12Si-8.5B-1.5Zr	3.48	1.93	555	14.1	
Mo-12Si-8.5B-3Zr	2.54	1.284	466	12.9	12.6 ± 0.5
Mo-12Si-8.5B-3Zr	2.76	1.149	416	12.2	

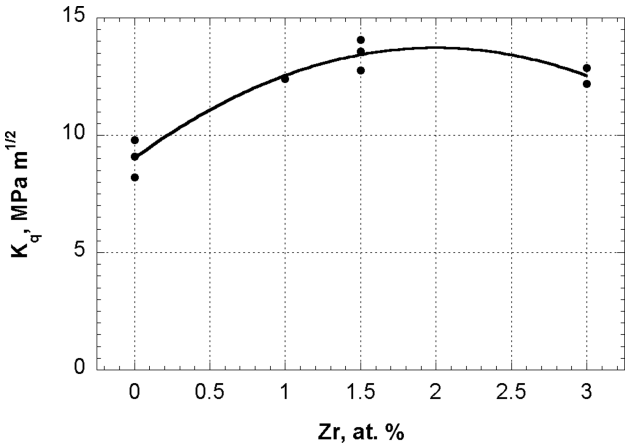

Fig. 8—Room-temperature fracture toughness of Mo-*x*Zr-12Si-8.5B as a function of the Zr concentration.

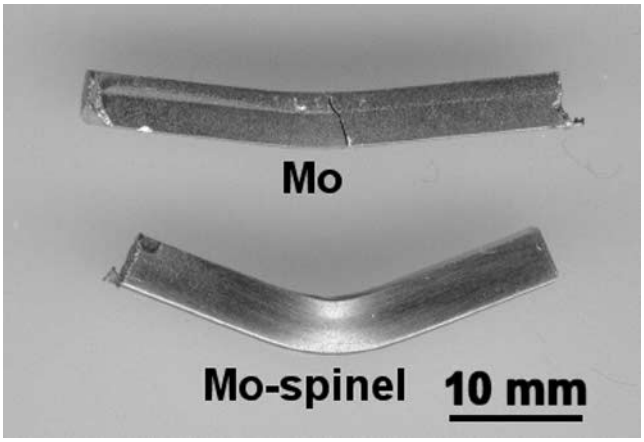

Fig. 9—Room-temperature flexure tests with Mo and Mo-9 vol pct $MgAl_2O_4$.

Mo reference specimen. While this result is encouraging, it needs to be viewed with caution. As Wadsworth *et al.*[26] point out, the ductility of Mo can vary widely depending on the C/O ratio and can reach values as high as 40 pct. In assessing the spinel ductilizing effect, it is of questionable value to use the ductility of "pure" molybdenum as a base line. The spinel ductilization effect will be more convincingly demonstrated if a regime can be found in which the ductility increases as the spinel volume fraction increases.

4. *Macroalloying with rhenium*

It is well established that the room-temperature ductility of Mo can be improved, and the ductile-to-brittle transition temperature reduced, by adding substantial (40 wt pct) amounts of Re. A recent review on this topic was given by Agnew and Leonhardt.[31] It is not known at this time how Re would partition into the different phases in Mo-Si-B, and whether they would remain stable. Also, whereas nominally pure Mo is ductilized by additions of Re, it is not known whether a Mo solid solution containing 2.5 at. pct Si would be ductilized. However, in view of the success of Mo-Re, it is worth assessing the effect of Re on the ductility and fracture toughness of Mo-Si-B alloys.

IV. CONCLUSIONS

When considering the suitability of Mo-Si-B–based materials for high-temperature structural applications, several property tradeoffs must be considered. We have illustrated that oxidation resistance and creep strength, on the one hand, and room-temperature fracture toughness, on the other, depend in opposite ways on the volume fraction of the α-Mo solid solution. In addition, factors such as morphology and size scale of the microstructure must be considered. The room-temperature fracture surface of a high-toughness Mo-Mo_3Si-Mo_5SiB_2 specimen indicated a substantial fraction of intergranular fracture of the Mo phase. The presence of intergranular fracture suggests that the ductility of the Mo phase, and thus its toughening efficiency, can be further increased. Several routes to do this have been presented; in particular, microalloying with Zr has been shown to be effective, and additions of $MgAl_2O_4$ spinel to Mo also hold promise. If the Mo phase can be ductilized sufficiently, adequate fracture toughness may be achieved with a smaller amount of α-Mo, and consequently, the oxidation resistance may be improved.

ACKNOWLEDGMENTS

One of the authors (JHS) acknowledges funding of this work by the Office of Fossil Energy, Advanced Research Materials (ARM) Program, WBS Element ORNL-2(I), and by the Division of Materials Sciences and Engineering, United States Department of Energy, under Contract No.

DE-AC05-00OR22725 with Oak Ridge National Laboratory, managed by UT–Battelle. ROR and JJK acknowledge funding by the Office of Fossil Energy, Advanced Research Materials Program, WBS Element LBNL-2, and by the Office of Science, Office of Basic Energy Sciences, Division of Materials Sciences and Engineering, United States Department of Energy, under Contract No. DE-AC03-76SF0098, with the Lawrence Berkeley National Laboratory.

REFERENCES

1. J.-C. Zhao and J.H. Westbrook: *MRS Bull.*, 2003, vol. 28 (9), p. 622 ff.
2. J.H. Schneibel, P.F. Tortorelli, M.J. Kramer, A.J. Thom, J.J. Kruzic, and R.O. Ritchie: *MRS Symposium Proceedings*, E.P. George, M.J. Mills, H. Inui, and G. Eggeler, eds., Materials Research Society, Warrendale, PA, 2003, vol. 753, pp. BB2.2.1-BB2.2.6.
3. D.M. Berczik: U.S. Patent No. 5,595,616, United Technologies Corp., East Hartford, CT, 1997.
4. D.M. Berczik: U.S. Patent No. 5,693,156, United Technologies Corp., East Hartford, CT, 1997.
5. C.A. Nunes, R. Sakidja, and J.H. Perepezko: in *Structural Intermetallics, 1997*, M.V. Nathal, R. Darolia, C.T. Liu, P.L. Martin, D.B. Miracle, R. Wagner, and M. Yamaguchi, eds., TMS, Warrendale, PA, 1997, pp. 831-39; also J.H. Perepezko, University of Wisconsin-Madison, Madison, WI, private communication, 2004.
6. I. Rosales and J.H. Schneibel: *Intermetallics*, 2000, vol. 8, pp. 885-89.
7. S. Katrych, A. Grytsiv, A. Bondar, P. Rogl, T. Velikanova, and M. Bohn: *J. Alloys Compounds*, 2002, vol. 347, pp. 94-100.
8. K. Ito, K. Ihara, K. Tanaka, M. Fujikura, and M. Yamaguchi: *Intermetallics*, 2001, vol. 9, pp. 591-602.
9. J.H. Schneibel and E.D. Specht: *Scripta Metall. Mater.*, 1994, vol. 31, pp. 1737-42.
10. J.H. Schneibel: *Intermetallics*, 2003, vol. 11, pp. 625-32.
11. J.H. Schneibel, M.J. Kramer, and D.S. Easton: *Scripta Mater.*, 2003, vol. 46, pp. 217-21.
12. M. Akinc, M.K. Meyer, M.J. Kramer, A.J. Thom, J.J. Huebsch, and B. Cook: *Mater. Sci. Eng. A*, 1999, vol. A261, pp. 16-23
13. J.H. Schneibel, C.T. Liu, D.S. Easton, and C.A. Carmichael: *Mater. Sci. Eng. A*, 1999, vol. A261, pp. 78-83.
14. J.H. Schneibel, D.S. Easton, H. Choe, and R.O. Ritchie: *Structural Intermetallics*, 3rd Int. Symp., K.J. Hemker and D.M. Dimiduk, eds., TMS, Warrendale, PA, 2001, pp. 801-09.
15. V. Supatarawanich, D.R. Johnson, and C.T. Liu: *Mater. Sci. Eng. A*, 2003, vol. A344, pp. 328-39.
16. J.B. Conway and P.N. Flagella: *Creep Rupture Data for the Refractory Metals to High Temperatures*, Gordon and Breach, New York, NY, 1971, p. 608.
17. J.H. Schneibel and H.T. Lin: *Mater High Temp.*, 2002, vol. 19, pp. 25-28.
18. J.H. Schneibel, M.J. Kramer, Ö. Ünal, and R.N. Wright: *Intermetallics*, 2001, vol. 9, pp. 25-31.
19. J.J. Kruzic, J.H. Schneibel, and R.O. Ritchie: *Scripta Mater.*, 2004, vol. 50, pp. 459-64.
20. A.Y. Koval, A.D. Vasilev, and S.A. Firstov: *Int. J. Refract. Alloys Hard Mater*, 1997, vol. 15, pp. 223-26.
21. H. Choe, J.H. Schneibel, and R.O. Ritchie: *Metall. Mater. Trans. A*, 2003, vol. 34A, pp. 225-39.
22. H. Choe, D. Chen, J.H. Schneibel, and R.O. Ritchie: *Intermetallics*, 2001, vol. 9, pp. 319-29.
23. R. Subramanian and J.H. Schneibel: *Acta Mater.*, 1998, vol. 46, pp. 4733-41.
24. M. Bannister and M.F. Ashby: *Acta Metall. Mater.*, 1991, vol. 39, pp. 2575-82.
25. A. Kumar and B.L. Eyre: *Proc. R. Soc. London*, 1980, vol. A370, pp. 431-58.
26. J. Wadsworth, T.G. Nieh, and J.J. Stephens: *Scripta Metall.*, 1986, vol. 20, pp. 637-42.
27. J.H. Schneibel, J.J. Kruzic, and R.O. Ritchie: *Proc. 17th Annual Conf. on Fossil Energy Materials*, Session III, National Energy Technology Laboratory (NETL) Publications, Washington, DC, 2003.
28. M.P. Brady, I.M. Anderson, M.L. Weaver, H.M. Meyer, L.R. Walker, M.K. Miller, D.J. Larson, I.G. Wright, V.K. Sikka, A. Rar, G.M. Pharr, J.R. Keiser, and C.A. Walls: *Mater. Sci. Eng. A*, 2003, vol. A358, pp. 243-54.
29. D.M. Scruggs, L.H. Van Vlack, and W.M. Spurgeon: *J. Am. Ceram. Soc.*, 1968, vol. 51, pp. 473-81.
30. D.M. Scruggs: U.S. Patent No. 3,320,036, Bendix Corporation, Southfield, MI, 1963.
31. S.R. Agnew and T. Leonhardt: *JOM*, 2003, Oct., pp. 25-29.